

# 公路建筑用铝合金表面激光熔覆 FeCoNiCr 高熵合金涂层的组织与抗腐蚀性

高珊珊, 李 刚, 都志强

(陕西铁路工程职业技术学院, 陕西渭南 714000)

**摘要:** 采用激光熔覆技术在铝合金表面制备FeCoNiCr高熵合金涂层, 研究该涂层的冶金质量、相结构、组织与电化学行为。结果表明: 当扫描速度为10 mm/s、激光功率300 W时, 容易产生未熔合主导的涂层缺陷; 400 W时可以得到高致密的涂层, 致密度高达99.6%; 而500 W时则导致气孔主导的涂层缺陷。当扫描速度为20 mm/s时, 不同激光功率的样品则产生以凝固裂纹为主的冶金缺陷。对致密的FeCoNiCr高熵合金涂层(扫描速度10 mm/s, 激光功率400 W)进行了组织表征及电化学测试, 结果表明, FeCoNiCr高熵合金涂层呈单相面心立方固溶体结构, 以柱状晶组织为主。晶粒内部存在大量的凝固胞状亚结构, 但是激光熔覆过程中, 极高的冷却速度抑制了凝固过程的元素偏析, Fe、Co、Ni、Cr均匀分布。极化曲线分析表明, 与铝合金基体相比, FeCoNiCr高熵合金涂层具有更高的腐蚀电位及更低的腐蚀电流密度, 表现出优异的抗腐蚀性能。

**关键词:** FeCoNiCr; 高熵合金涂层; 激光熔覆; 组织; 腐蚀

铝合金导电性、导热性优异, 密度低, 比强度高, 广泛应用于汽车、航空、公路等领域<sup>[1]</sup>。此外, 铝合金具有优良的抗腐蚀性, 广泛应用于化工设备, 如过滤器、分馏塔等。铝合金优良的抗腐蚀性源自保护性氧化膜的形成; 然而, 铝合金在氯离子的环境中, 保护性氧化膜会加速破坏, 不能起到有效保护作用, 极易发生点蚀<sup>[2-3]</sup>。例如, 高速公路护栏用铝合金使用短短几年便可能锈迹斑斑; 尤其在沿海城市及重工业区, 大气中的氯离子浓度更高, 会加速铝合金的腐蚀。通常腐蚀发生在材料表面, 因此可以通过形成表面保护层来改善铝合金在氯离子环境中的抗腐蚀性。目前多种涂层, 包括钛合金涂层<sup>[2]</sup>、金属基复合材料<sup>[1, 4-5]</sup>、有机涂层<sup>[3, 6-8]</sup>、陶瓷涂层<sup>[9-12]</sup>、碳纳米管涂层<sup>[13]</sup>用以改善铝合金的抗腐蚀性。与传统合金截然不同, 高熵合金通常含有多种元素, 且这些元素以等原子比或近等原子比存在<sup>[14]</sup>。高熵合金的发现, 极大地扩展了合金的成分区间, 使合金的研发不再依赖于单一主元, 而向多种主元合金扩展。尽管高熵合金含有多种主元, 但是由于高的组态熵效应, 高熵合金通常形成无序面心立方、体心立方或者密排六方的固溶体结构<sup>[15-16]</sup>。此外, 高熵合金晶格畸变极其严重<sup>[17]</sup>, 且具有鸡尾酒效应<sup>[18]</sup>。高熵合金这样独特的成分及结构特点导致其具有某些优异的性能, 如低温韧性<sup>[15]</sup>和耐腐蚀性能<sup>[19]</sup>。FeCoNiCr高熵合金为典型的单相面心立方结构高熵合金, 与铝合金基体的晶体结构一致, 可以提高二者之间的结合力。此外, 面心立方结构FeCoNiCr与激光加工技术具有良好的兼容性<sup>[27]</sup>, 更容易获得高质量的涂层。目前已经有研究者关注到在铝合金表面制备高熵合金涂层, 提高表面的抗腐蚀性及耐磨性<sup>[20-26]</sup>。

本研究以1050铝合金作为基体材料, 利用激光熔覆技术在其表面制备FeCoNiCr高熵合金涂层, 通过工艺参数优化, 有效抑制了可能存在的冶金缺陷(如局部未熔合、气孔、裂纹), 得到了致密的FeCoNiCr高熵合金涂层, 并对其相组成、组织及电化学行为进行了研究。

作者简介:

高珊珊(1985-), 女, 硕士, 讲师, 研究方向为金属材料激光表面改性。电话: 18691521688, E-mail: gaoshanshan198512@163.com

中图分类号: TG146.2

文献标识码: A

文章编号: 1001-4977(2022)

07-0839-06

收稿日期:

2021-11-16 收到初稿,

2022-01-02 收到修订稿。

## 1 试验材料与方法

试验中选用的基体材料为1050铝合金，铝合金基体用400、600、800、1 200号砂纸依次打磨，并用丙酮除油，无水乙醇除水并风干。成形粉末为旋转电极雾化方法制备的FeCoNiCr高熵合金粉末，如图1所示。球形粉末尺寸在40~120  $\mu\text{m}$ 之间，无卫星粉形成，这对保证粉末的流动性至关重要。此外，粉末表面光滑，表明无氧化发生。激光熔覆过程中，高功率激光直接作用于铝合金基体表面，形成一个熔池。FeCoNiCr高熵合金粉末跟随氩气，从喷嘴中喷出，进入熔池内。样品台沿x-y方向运动，便可制备一层涂层。激光熔覆在氩气的保护气氛下进行，氧含量低于 $20 \times 10^{-6}$ ，以避免氧化。激光熔覆过程中，改变激光功率及扫描速度，研究其对FeCoNiCr高熵合金涂层冶金缺陷及致密度的影响，其他参数为开口间距450  $\mu\text{m}$ ，送粉速度23 g/min。

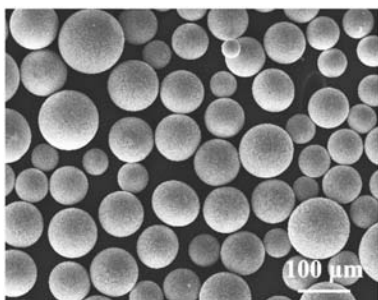


图1 FeCoNiCr高熵合金粉末形貌

Fig. 1 Morphology of FeCoNiCr high-entropy alloy powders

激光熔覆FeCoNiCr涂层经线切割、研磨、抛光制备成金相试样。采用光学显微镜(OM, Leica)对涂层内部的冶金缺陷进行分析，并用ImageJ软件对涂层的致密度进行统计分析。采用10%的磷酸溶液对金相试样进行电解腐蚀，利用OM及扫描电子显微镜(SEM, Quanta400)观察各类冶金缺陷的形貌。对致密的FeCoNiCr涂层进行进一步的组织分析及电化学行为研究。利用X射线衍射仪(XRD, Bruker)对激光熔

覆FeCoNiCr高熵合金涂层的组成相进行分析，利用电子背散射衍射技术(EBSD)对激光熔覆FeCoNiCr涂层的晶粒结构进行分析。EBSD样品经过打磨后，用1  $\mu\text{m}$ 的金刚石抛光液进行抛光，最后用20 nm的胶体氧化硅溶液进行最终抛光。利用透射电子显微镜(TEM, JEOL-2100F)对FeCoNiCr涂层的显微组织进行分析，并利用能谱(EDS)对元素分布进行分析。TEM样品采用机械研磨的方法减薄至50  $\mu\text{m}$ ，冲出直径为3 mm的小圆片，并通过双喷电解抛光的方法进行制备。极化曲线在三电极系统的电化学工作站上进行，参比电极采用Ag/AgCl电极，辅助电极采用Pt片，工作电极为FeCoNiCr涂层，采用3.5wt.% NaCl溶液为腐蚀溶液。

## 2 试验结果与讨论

### 2.1 激光熔覆 FeCoNiCr 高熵合金涂层的冶金缺陷

激光熔覆FeCoNiCr高熵合金涂层的冶金缺陷见图2，在所采用的激光加工参数范围内，观察到三类冶金缺陷，即局部未熔合、气孔和微裂纹。当扫描速度为10 mm/s、激光功率为300 W时，样品中出现形状不规则的孔洞，孔洞尺寸较大，可达200  $\mu\text{m}$ 以上(图2a)。样品经腐蚀后，可以明显看到，这些形状不规则的孔洞出现在层间(图3a)，该类缺陷为局部未熔合缺陷。局部未熔合缺陷的形成可归因于激光功率过低，热输入不足，导致层间重熔不足而未能达到良好的冶金结合。当激光功率提高至400 W时，局部未熔合缺陷完全消失，得到致密的FeCoNiCr涂层样品(图2b)。当激光功率进一步增加至500 W时，样品中再次出现明显的孔洞(图2c)。与图2a中的未熔合缺陷不同，图2c中样品的孔洞为近似球形，且尺寸更小，一般低于50  $\mu\text{m}$ 。样品经腐蚀后，可以看出，该球形孔洞主要位于熔池底部(图3b)。该类孔洞为气孔，与局部未熔合缺陷形成机制不同。一般而言，激光加工过程有两种传热模式，一种为导热模式，一种为锁孔模式。当激光功率过高，或扫描速度过慢时，热输入极

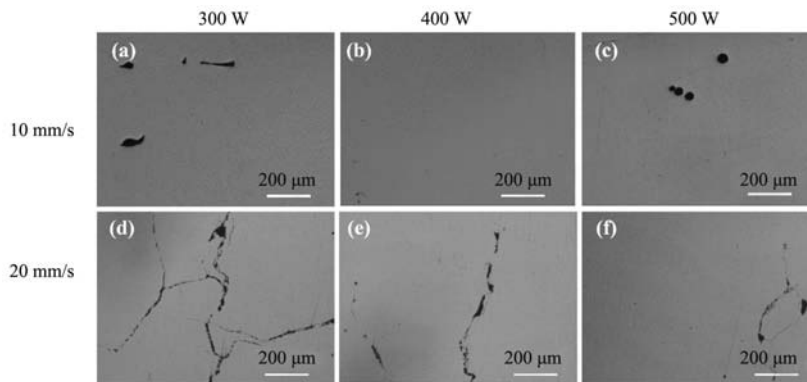


图2 激光熔覆FeCoNiCr高熵合金涂层的冶金缺陷

Fig. 2 Metallurgy defects of laser-cladded FeCoNiCr high-entropy alloy

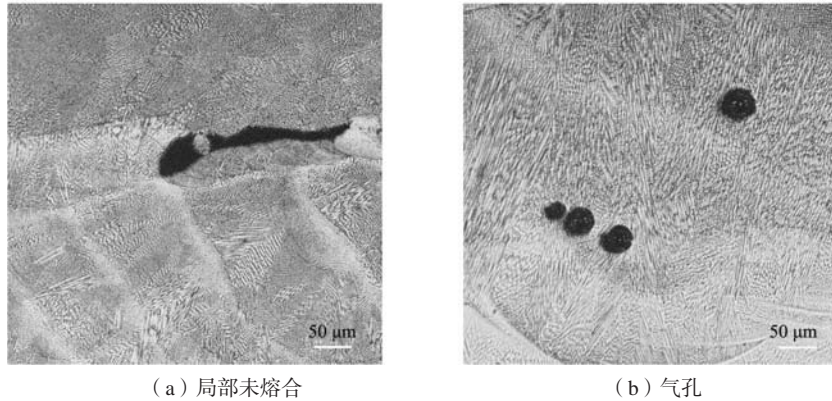


图3 激光熔覆FeCoNiCr高熵合金涂层的典型的冶金缺陷

Fig. 3 Typical metallurgy defects of laser-cladded FeCoNiCr high-entropy alloy

大，熔池形状窄而深，即传热模式由导热向锁孔模式转变，该种模式极易在熔池底部形成气孔。

与扫描速度为10 mm/s的样品不同，扫描速度为20 mm/s的样品冶金缺陷均以微裂纹为主（图2d-e）。一般而言，激光加工过程中合金的开裂分为四种，即应变时效开裂<sup>[28]</sup>、失延开裂<sup>[29-30]</sup>、液化开裂<sup>[31-33]</sup>及凝固开裂<sup>[34-35]</sup>。应变时效开裂多出现在析出强化型合金中，当熔池凝固结束后，在合金冷却过程中析出大量的沉淀强化相，与残余应力共同作用下，导致合金塑性降低，产生开裂<sup>[28]</sup>。失延开裂类似，也多发生在熔池凝固结束后的冷却过程中，由于合金的塑性降低，导致开裂<sup>[29-30]</sup>。值得注意的是，应变时效开裂与失延开裂均发生在合金凝固后的冷却阶段，属于固态下产生的裂纹。通过SEM观察发现，在扫描速度为20 mm/s的样品中，裂纹内部具有枝晶形貌（图4），由此可以判断，该裂纹形成时存在液相膜，因而排除应变时效开裂与失延开裂两种开裂机制。液化裂纹多形成于热影响区，由于激光热循环作用，导致热影响区某些低熔点共晶化合物熔化，在随后凝固过程中，由于收缩力的作用导致开裂<sup>[31-33]</sup>。本研究的FeCoNiCr为典型的单相面心立方结构的高熵合金，并不存在低熔点共晶，

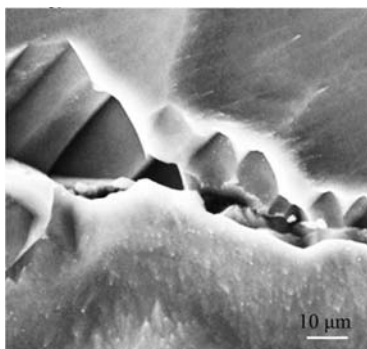


图4 激光熔覆FeCoNiCr高熵合金涂层典型的微裂纹SEM图像  
Fig. 4 A typical SEM micrograph of microcrack of the laser-cladded FeCoNiCr high-entropy alloy

所以排除液化开裂。综合以上的讨论，本研究中的微裂纹为凝固裂纹，即在凝固后期，固相分数已经足够大，邻近的枝晶相互接触，当残余液相凝固收缩时，额外的液相无法进入收缩区域进行补缩而形成微孔，在残余应力的作用下，形成微裂纹。众所周知，当激光扫描速度增加时，熔池内部的温度梯度相应增大，残余应力增大，故凝固开裂倾向增大。图5为不同激光加工参数样品的致密度统计结果，可见，当激光功率为400 W、扫描速度为10 mm/s时，FeCoNiCr涂层最为致密，孔隙率仅为0.4%。因此，针对该涂层做进一步的组织表征及电化学测试。

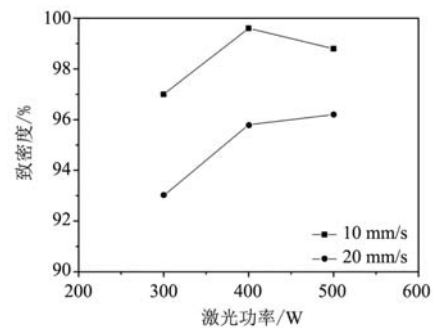


图5 激光加工参数对FeCoNiCr高熵合金涂层致密度的影响  
Fig. 5 Effect of laser processing parameters on the relative density of FeCoNiCr high-entropy alloy

## 2.2 激光熔覆 FeCoNiCr 高熵合金涂层的显微组织及电化学行为

图6给出了激光熔覆FeCoNiCr高熵合金涂层的XRD图谱，从图中可以看出，FeCoNiCr涂层为单相面心立方组织。图7为激光熔覆FeCoNiCr高熵合金涂层EBSD反极图面分布图，可以看出，该涂层为典型的柱状晶组织，仅有少量的等轴晶存在，柱状晶大致垂直向上生长。在晶粒内部存在大量的凝固胞状亚结构，如图8所示。胞状亚结构的存在表明，胞状凝固控制激光熔覆过程。从图8也可以看出，在胞状亚结构内部位错密度极低，而在胞壁存在大量的位错，表明胞状亚结构



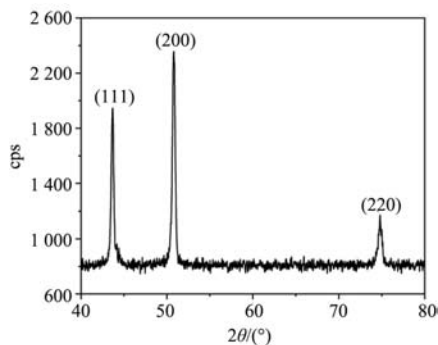


图6 激光熔覆FeCoNiCr高熵合金涂层XRD图谱

Fig. 6 XRD pattern of the laser-clad FeCoNiCr high-entropy alloy coating

的本质为位错胞。EDS扫描的结果表明,胞状亚结构上并不存在明显的元素偏析,Fe、Co、Ni、Cr均匀分布在胞壁及胞内。

图9为FeCoNiCr涂层与铝合金基体的极化曲线,腐蚀溶液为3.5wt.% NaCl溶液。从图中可以看出,铝

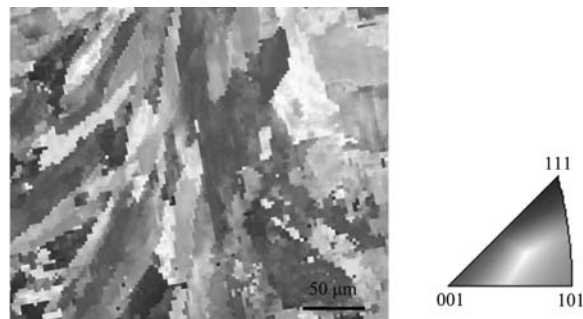


图7 激光熔覆FeCoNiCr高熵合金涂层EBSD反极图面分布图

Fig. 7 EBSD inverse pole figure (IPF) map of laser-clad FeCoNiCr high-entropy alloy coating

合金基体的腐蚀电位为-0.596 V, FeCoNiCr涂层的腐蚀电位提高至-0.116 V。此外,与铝合金基体相比,FeCoNiCr高熵合金涂层的腐蚀电流密度降低三个数量级。从极化曲线来看,铝合金基体没有明显的钝化阶段,而FeCoNiCr表现出明显的钝化平台,即随着

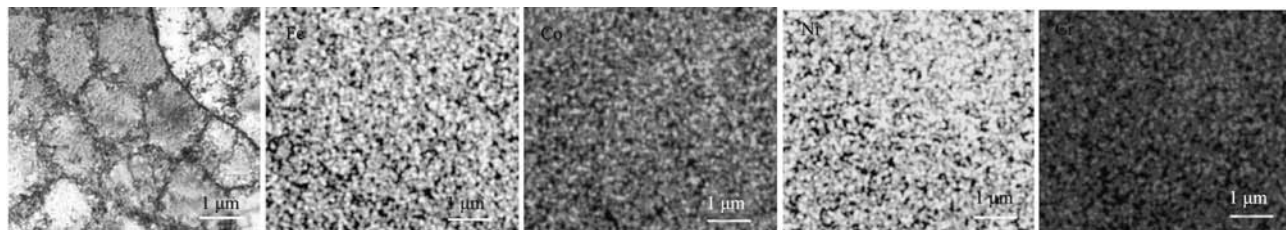


图8 激光熔覆FeCoNiCr高熵合金涂层中的位错胞及元素分布

Fig. 8 Dislocation cells and elemental distribution of laser-clad FeCoNiCr high-entropy alloy coating

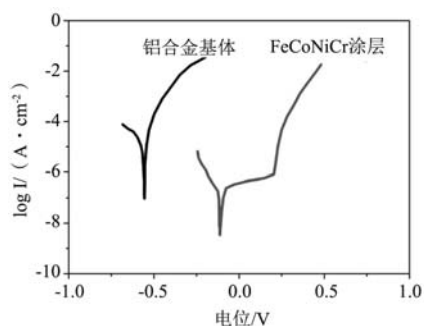


图9 铝合金基体与FeCoNiCr高熵合金涂层的极化曲线

Fig. 9 Polarization curves of aluminum alloy substrate and FeCoNiCr high-entropy alloy coating

电位的升高,电流密度几乎保持不变。显然,与铝合金基体相比,激光熔覆FeCoNiCr高熵合金涂层在3.5wt.% NaCl溶液中的腐蚀抗力得到明显提高。此外,激光熔覆FeCoNiCr高熵合金涂层在3.5wt.% NaCl溶液中的腐蚀电位高于其他高熵合金涂层的腐蚀电位,如AlCoCrFeNiTi<sub>x</sub> (-0.5~-0.4 V)<sup>[36]</sup>, AlCoCrFeNiSi (-0.33 V)<sup>[37]</sup>, Al<sub>2</sub>CrFeCo<sub>x</sub>CuNiTi (-0.7~-0.2 V)<sup>[38]</sup>,表现极其优异的抗腐蚀性能。腐蚀抗力提高可能有以下几种原因:首先,在Cl<sup>-</sup>离子的腐蚀溶液中,铝合金基体通常的腐蚀模式为点蚀。而通过在铝合金基体上

制备FeCoNiCr高熵合金涂层,由于涂层中含有大量的Cr元素,且激光熔覆过程中高的冷却速度抑制凝固偏析动力学,导致Cr元素均匀分布,可以促进均匀钝化膜的形成,有效保护铝合金基体免受侵蚀。此外,由于FeCoNiCr涂层本身的高熵效应,FeCoNiCr合金涂层形成极细的简单面心立方结构的组织,也可以有效降低由于形成原电池而导致的加速腐蚀效应<sup>[39]</sup>。

### 3 结论

(1) 当扫描速度为10 mm/s、激光功率300 W时,容易产生未熔主导涂层缺陷,400 W可以得到高致密的涂层,而500 W时则导致气孔主导的涂层缺陷。当扫描速度为20 mm/s时,不同激光功率的样品则产生以凝固裂纹为主的冶金缺陷。

(2) FeCoNiCr高熵合金涂层呈单相面心立方固溶体结构,以柱状晶组织为主。晶粒内部存在大量的凝固胞状亚结构,但是激光熔覆过程中极高的冷却速度抑制了凝固过程的元素偏析,Fe、Co、Ni、Cr均匀分布。

(3) 与铝合金基体相比,FeCoNiCr高熵合金涂层具有更高的腐蚀电位及更低的腐蚀电流密度,表现出优异的抗腐蚀性能。

## 参考文献:

- [1] FRANCO M, SHA W, TAN V, et al. Insight of the interface of electroless Ni-P/SiC composite coating on aluminium alloy LM24 [J]. *Materials & Design*, 2015, 85: 248–255.
- [2] SUN Y. Thermally oxidised titanium coating on aluminium alloy for enhanced corrosion resistance [J]. *Materials Letters*, 2004, 58 ( 21 ) : 2635–2639.
- [3] VIGNESH R B, BALAJI J, SETHURAMAN M G. Surface modification, characterization and corrosion protection of 1, 3-diphenylthiourea doped sol-gel coating on aluminium [J]. *Progress in Organic Coatings*, 2017, 111: 112–123.
- [4] SOLEIMANI R, MAHBOUBI F, KAZEMI M, et al. Corrosion and tribological behaviour of electroless Ni-P/nano-SiC composite coating on aluminium 6061 [J]. *Surface Engineering*, 2015, 31 ( 9 ) : 714–721.
- [5] REDDY G M, RAO K S, MOHANDAS T. Friction surfacing: novel technique for metal matrix composite coating on aluminium-silicon alloy [J]. *Surface Engineering*, 2009, 25 ( 1 ) : 25–30.
- [6] HIKKU G S, JEYASUBRAMANIAN K, VENUGOPAL A, et al. Corrosion resistance behaviour of graphene/polyvinyl alcohol nanocomposite coating for aluminium-2219 alloy [J]. *Journal of Alloys and Compounds*, 2017, 716: 259–269.
- [7] DALMORO V, ALEMÁN C, FERREIRA C A, et al. The influence of organophosphonic acid and conducting polymer on the adhesion and protection of epoxy coating on aluminium alloy [J]. *Progress in Organic Coatings*, 2015, 88: 181–190.
- [8] ROBERT R B J, HIKKU G S, JEYASUBRAMANIAN K, et al. ZnO nanoparticles impregnated polymer composite as superhydrophobic anti-corrosive coating for Aluminium-6061 alloy [J]. *Materials Research Express*, 2019, 6 ( 7 ) : 075705.
- [9] BOSTA M M S, MA K J, CHIEN H H. The effect of MAO processing time on surface properties and low temperature infrared emissivity of ceramic coating on aluminium 6061 alloy [J]. *Infrared Physics & Technology*, 2013, 60: 323–334.
- [10] YUE T M, HUANG K J, MAN H C. Laser cladding of Al<sub>2</sub>O<sub>3</sub> coating on aluminium alloy by thermite reactions [J]. *Surface and Coatings Technology*, 2005, 194 ( 2-3 ) : 232–237.
- [11] XIN S G, SONG L X, ZHAO R G, et al. Properties of aluminium oxide coating on aluminium alloy produced by micro-arc oxidation [J]. *Surface and Coatings Technology*, 2005, 199 ( 2-3 ) : 184–188.
- [12] BOSTA M M S, MA K J. Suggested mechanism for the MAO ceramic coating on aluminium substrates using bipolar current mode in the alkaline silicate electrolytes [J]. *Applied Surface Science*, 2014, 308: 121–138.
- [13] THEOCHAROUS E, CHUNNILALL C J, MOLE R, et al. The partial space qualification of a vertically aligned carbon nanotube coating on aluminium substrates for EO applications [J]. *Optics Express*, 2014, 22 ( 6 ) : 7290–7307.
- [14] YEH J W, CHEN S K, LIN S J, et al. Nanostructured high-entropy alloys with multiple principal elements: novel alloy design concepts and outcomes [J]. *Advanced Engineering Materials*, 2004, 6 ( 5 ) : 299–303.
- [15] GLUDOVATZ B, HOHENWARTER A, CATOOR D, et al. A fracture-resistant high-entropy alloy for cryogenic applications [J]. *Science*, 2014, 345 ( 6201 ) : 1153–1158.
- [16] ZOU Y, MAITI S, STEURER W, et al. Size-dependent plasticity in an Nb<sub>25</sub>Mo<sub>25</sub>Ta<sub>25</sub>W<sub>25</sub> refractory high-entropy alloy [J]. *Acta Materialia*, 2014, 65: 85–97.
- [17] KÖRMANN F, SLUITER M. Interplay between lattice distortions, vibrations and phase stability in NbMoTaW high entropy alloys [J]. *Entropy*, 2016, 18: 1–7.
- [18] PICKERING E J, JONES N G. High-entropy alloys: a critical assessment of their founding principles and future prospects [J]. *International Materials Reviews*, 2016, 61 ( 3 ) : 183–202.
- [19] THAPLIYAL S, NENE S S, AGRAWAL P, et al. Damage-tolerant, corrosion-resistant high entropy alloy with high strength and ductility by laser powder bed fusion additive manufacturing [J]. *Additive Manufacturing*, 2020, 36: 101455.
- [20] NI C, SHI Y, LIU J, et al. Characterization of Al<sub>0.5</sub>FeCu<sub>0.7</sub> NiCoCr high-entropy alloy coating on aluminum alloy by laser cladding [J]. *Optics & Laser Technology*, 2018, 105: 257–263.
- [21] ZUO H, WANG L, GONG M, et al. Corrosion behavior of ZrCrMoNb high-entropy alloy coating in ethylene glycol solution [J]. *International Journal of Electrochemical Science*, 2021, 16: 150912.
- [22] KATAKAM S, JOSHI S S, MRIDHA S, et al. Laser assisted high entropy alloy coating on aluminum: Microstructural evolution [J]. *Journal of Applied Physics*, 2014, 116 ( 10 ) : 104906.
- [23] LI Y, SHI Y. Phase assemblage and properties of laser clad Ti<sub>1</sub>CrFeCoNiCu high-entropy alloy coating on aluminum [J]. *Materials Research Express*, 2020, 7 ( 3 ) : 036519.
- [24] ZHAO D, YAMAGUCHI T, SHU J, et al. Rapid fabrication of the continuous AlFeCrCoNi high entropy alloy coating on aluminum alloy by resistance seam welding [J]. *Applied Surface Science*, 2020, 517: 145980.
- [25] ZHANG H, PAN Y, HE Y Z. Synthesis and characterization of FeCoNiCrCu high-entropy alloy coating by laser cladding [J]. *Materials & Design*, 2011, 32 ( 4 ) : 1910–1915.
- [26] ARGADE G R, JOSHI S S, AYYAGARI A V, et al. Tribocorrosion performance of laser additively processed high-entropy alloy coatings

- on aluminum [J]. Applied Physics A, 2019, 125 (4) : 1–9.
- [27] BRIFY, THOMAS M, TODD I. The use of high-entropy alloys in additive manufacturing [J]. Scripta Materialia, 2015, 99: 93–96.
- [28] ASAVAVISITHCHAI S, HOMKRAJAI W, WANGYAO P. Strain-age cracking after postweld heat treatments in Inconel 738 superalloy [J]. High Temperature Materials and Processes, 2010, 29: 61–67.
- [29] RAMIREZ A J, LIPPOLD J C. High temperature behavior of Ni-base weld metal: part II. insight into the mechanism for ductility dip cracking [J]. Materials Science and Engineering A, 2004, 380 (1) : 245–258.
- [30] NÉMETH A A N, CRUDDEN D J, ARMSTRONG D E J, et al. Environmentally-assisted grain boundary attack as a mechanism of embrittlement in a nickel-based superalloy [J]. Acta Materialia, 2017, 126: 361–371.
- [31] OJO O A, RICHARDS N L, CHATURVEDI M C. Contribution of constitutional liquation of gamma prime precipitate to weld HAZ cracking of cast Inconel 738 superalloy [J]. Scripta Materialia, 2004, 50 (5) : 641–646.
- [32] OJO O A, RICHARDS N L, CHATURVEDI M C. Study of the fusion zone and heat-affected zone microstructures in tungsten inert gas-welded INCONEL 738LC superalloy [J]. Metallurgical and Materials Transactions A, 2006, 37 (2) : 421–433.
- [33] ZHONG M, SUN H, LIU W, et al. Boundary liquation and interface cracking characterization in laser deposition of Inconel 738 on directionally solidified Ni-based superalloy [J]. Scripta Materialia, 2005, 53 (2) : 159–164.
- [34] HAN Q Q, MERTENS R, MONTERO-SISTIAGA M L, et al. Laser powder bed fusion of Hastelloy X: effects of hot isostatic pressing and the hot cracking mechanism [J]. Materials Science and Engineering A, 2018, 732: 228–239.
- [35] WANG L, WANG N, PROVATAS N. Liquid channel segregation and morphology and their relation with hot cracking susceptibility during columnar growth in binary alloys [J]. Acta Materialia, 2017, 126: 302–312.
- [36] LIU J, LIU H, CHEN P, et al. Microstructural characterization and corrosion behaviour of AlCoCrFeNiTi<sub>x</sub> high-entropy alloy coatings fabricated by laser cladding [J]. Surface and Coatings Technology, 2019, 361: 63–74.
- [37] ZHANG G, LIU H, TIAN X, et al. Microstructure and properties of AlCoCrFeNiSi high-entropy alloy coating on AISI 304 stainless steel by laser cladding [J]. Journal of Materials Engineering and Performance, 2020, 29 (1) : 278–288.
- [38] QIU X W. Corrosion behavior of Al<sub>2</sub>CrFeCo<sub>2</sub>CuNiTi high-entropy alloy coating in alkaline solution and salt solution [J]. Results in Physics, 2019, 12: 1737–1741.
- [39] SHI Y, YANG B, LIAW P K. Corrosion-resistant high-entropy alloys: a review [J]. Metals, 2017, 7 (2) : 1–18.

## Microstructure and Corrosion Resistance of Laser-Cladded FeCoNiCr High-Entropy Alloy Coating on Aluminum Alloys for Highway Architecture Applications

GAO Shan-shan, LI Gang, DU Zhi-qiang  
(Shaanxi Railway Institute, Weinan 714000, Shaanxi, China)

### Abstract:

Laser cladding was used to deposit FeCoNiCr high-entropy alloy coating on the aluminum alloy substrate, and the metallurgical quality, phase structure, microstructure and electrochemical behavior were investigated. The results showed that when the scan speed was 10 mm/s; a laser power of 300 W easily produced lack-of-fusion dominated coating defects, a laser power of 400 W achieved highly dense coatings, with the densification of 99.6%; whereas a laser power of 500 W led to the formation of gas pores dominated coating defects. When the laser power was 20 mm/s, the coatings deposited at various laser powers were dominated by solidification cracks. The microstructural characterization and electrochemical testing were performed on the dense FeCoNiCr high-entropy alloy coating (scan speed 10 mm/s, laser power 400 W), and the results showed that the FeCoNiCr high-entropy alloy has a single-phase face-centered-cubic structure, and the grain structure was dominated by columnar grains. Within the grains, numerous solidification cell substructures existed, and Fe, Co, Ni, and Cr were uniformly distributed due to the ultrahigh cooling rate and the prohibited solidification segregation kinetics. Polarization curves showed that as compared with the aluminum alloy substrate, FeCoNiCr high-entropy alloy coating exhibited a higher corrosion potential and a lower corrosion current density, and hence an improved corrosion resistance.

### Key words:

FeCoNiCr; high-entropy alloy coating; laser cladding; microstructure; corrosion